ChemComm

Accepted Manuscript

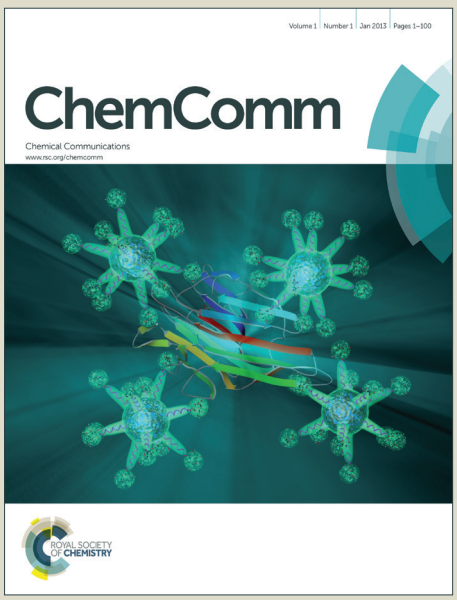

ROYAL SOCIETY OF CHEMISTRY

www.rsc.org/chemcomm

ChemComm

RSCPublishing

COMMUNICATION

Template-directed construction of conformational supramolecular isomers for bilayer porous metal–organic frameworks with distinct gas sorption behaviors†

Cite this: DOI: 10.1039/xoxxoooooox

Received ooth xxxx xxxx,
Accepted ooth xxxx xxxx

DOI: 10.1039/xoxxoooooox

www.rsc.org/

Min Chen,[a] Hui Zhao,[a] Chun-Sen Liu,[a] Xi Wang,[ab] Heng-Zhen Shi*[a] and Miao Du*[ab]

A pair of supramolecular isomers of Co(II)-based metal–organic frameworks can be directionally constructed in virtue of solvent templates, which show diverse bilayer networks and lattice packing with the same Co_3 SBUs and organic linkers. The two porous materials show distinct gas sorption behaviors at different temperatures, especially their CO_2 sorption selectivity.

Metal–organic frameworks (MOFs) are a new class of crystalline porous materials, which have great potentials in various applications such as gas storage and separation,[1] magnetism,[2] catalysis[3] and drug delivery.[4] Since the properties of MOFs will be mainly influenced by their compositions and a series of structural features, the comparison of structure-functionality differences for isomeric MOFs can provide a nice platform for profoundly understanding the intrinsic structure-functionality relationship.[5–9] Supramolecular isomerism or polymorphism for coordination networks refers to the existence of different architectures with the same building blocks (metal ions and organic linkers) and identical stoichiometry, which can be classified to structural, conformational, catenane, and optical isomerism.[10] Normally, the flexible ligands can engender conformational changes to generate different but often related networks, namely, conformational isomerism.[10] The changes in spatial and linking arrangements of the spacers in such isomers may be induced by temperature,[5] reaction time,[6] and template (solvent,[7] auxiliary neutral molecule,[8] or anion[9]) effect. The structural features of pores, such as their sizes, shapes, and environments, have been found to play an important role in designing MOFs with different functional applications. Generally, the pores of MOFs will be initially filled with solvent guests used in synthesis. Thus, the structures and chemical properties of such template molecules can be transcribed into the resulting porous characteristics. In this work, we used 4,4',4''-(benzene-1,3,5-triyl-tris(oxy))tribenzoic acid (H_3BTTB), bearing three flexible rotatable –O– motifs, to successfully construct a pair of conformational supramolecular isomers directed by solvent templates, which show significantly different gas sorption behaviors.

In a typical synthesis, single crystals of 470-MOF (Fig. S1, ESI†) were obtained by heating a 1:2 mixture of H_3BTTB and $CoCl_2 \cdot 6H_2O$ at 120 °C for 72 h in DMF. Similarly, 471-MOF (Fig. S1, ESI†) can be synthesized by adding 1,4-diethylene dioxide during this reaction. The phase purity for bulk materials was confirmed by powder X-ray diffraction (PXRD, see Fig. S2, ESI†). Based on thermogravimetric analysis (TGA, Fig. S3, ESI†) and elemental analysis (ESI†), the two materials were formulated as $[Co_3(BTTB)_2(H_2O)_2]\cdot(DMF)_{4.5}\cdot(H_2O)_4$ for 470-MOF and $[Co_3(BTTB)_2(H_2O)_2]\cdot(DMF)_3\cdot(H_2O)_4\cdot(dioxane)_{2.5}$ for 471-MOF, respectively. Obviously, the solvent molecules act as the templates and play an important role in controlling the supramolecular isomerism in this case.

Single-crystal X-ray diffraction analysis indicates that 470-MOF and 471-MOF crystallize in the trigonal *P*-31*c* and *R*-3*c* space group (see Table S1, ESI†), respectively. Interestingly, both materials have the same framework formula but with different lattice guest solvents, which thus can be classified as a pair of supramolecular isomers. The asymmetric coordination units for both structures contain two independent Co(II) ions (with 1/3 and 1/6 occupancy, respectively), 1/3 BTTB ligand, and one water ligand with 1/3 occupancy (see Fig. S4, ESI†). In each structure, the Co1 center is octahedrally coordinated to six oxygen atoms from the bridging carboxylate groups of six BTTB ligands, while the tetrahedral sphere of Co2 is fulfilled by three oxygen atoms from the bridging carboxylates of three BTTB ligands and one terminal water ligand. The axial Co–O_{water} length for the CoO_4 tetrahedron in 470-MOF (2.203(2) Å) is markedly stretched in comparison with that in 471-MOF (2.080(8) Å). Moreover, two pairs of triple carboxylate bridges are further converged to the central Co1 and two terminal Co2 atoms to give a trinuclear $[Co_3(O_2CR)_6(H_2O)_2]$ SBU. The Co1···Co2 distances are 3.61 and 3.60 Å in 470-MOF and 471-MOF, respectively, and such three Co(II) centers are collinear in both structures, where each μ_2-carboxylate group of the fully deprotonated BTTB ligand connects two Co(II) ions (Fig. S5, ESI†). The dihedral angles between three sloping benzene arms and the central benzene group in BTTB are 71.3° for 470-MOF and 83.0° for 471-MOF (Figs. 1a and 1f), as a result of different extending fashions for the isomeric networks. The isomerism also arises from the symmetry of Co_3 SBUs (see Figs. 1b and 1g). In fact, the Co_3 SBUs in both 470-

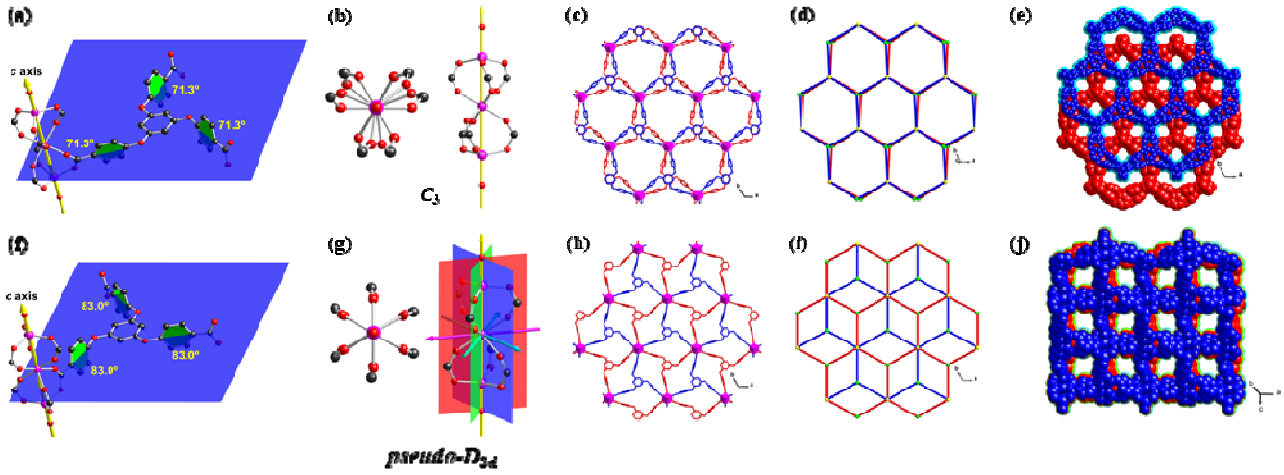

Fig. 1 Crystal structures for 470-MOF (a–e) and 471-MOF (f–j). (a, f) View of the arrangements for three sloping benzene arms around the central benzene ring. (b, g) View of the conformation of trimeric Co(II) SBU. (c, h) View of the 2-D bilayer network along *c*-axis, where the "up" and "down" ligands are shown with blue and red colors, respectively. (d, i) Schematic view of the (3,6)-connected 2-D network with the Schläfli symbol of $(4^3.6^{12})(4^3)_2$ or $(4^3)_2(4^6.6^6.8^3)$. (e, j) Space-filling view of the 3-D lattice packing showing the 1-D channels.

MOF and 471-MOF have the C_3 proper rotational axis along *c*-axis (Figs. 1b and 1g). On one hand, no other symmetry element exists in the Co_3 SBU for 470-MOF to result in its C_3 symmetry (see Fig. 1b), where the dihedral angles between the carboxylates range from 20.1 to 83.2° (Fig. S6a and Table S3, ESI†). On the other hand, the carboxylates of Co_3 SBU for 471-MOF almost divide the circle equally, with their limited dihedral angles of 59.5–60.0° (Fig. S6b and Table S4, ESI†), which thus possesses the *pseudo-*D_{3d} symmetry with three C_2 counter shafts and σ_d mirror faces (see Fig. 1g). Though each Co_3 SBU is linked to six other Co_3 SBUs through six 3-connected BTTB ligands in both isomers (Fig. S7, ESI†), distinct 2-D (3,6)-connected bilayer networks are observed parallel to the *ab* plane, with the "up" and "down" linkers (Figs. 1c, 1d, 1h, and 1i). This difference can be attributed to the conformational diversity for BTTB ligands and Co_3 SBUs in two isomers. The resultant 2-D layer shows hexagonal pores with approximate dimensions of 13.0 × 13.0 Å^2 (distance of Co···Co after considering the van der Waals radii) in 470-MOF (see Fig. 1c), whereas that in 471-MOF consists of distorted quadrangular meshes with the sizes of 14.0 × 2.0 Å^2 (distances of Co···Co and the shorter O···O of ether groups after considering the van der Waals radii) (see Fig. 1h). From the topological viewpoint, the Co_3 SBUs and BTTB ligands can be considered as the 6-connected and 3-connected nodes, respectively. Consequently, such 2-D bilayers can be simplified as a (3,6)-connected MoS_2-H net (with Schläfli symbol of $(4^3{\cdot}6^{12})(4^3)_2)$[11] for 470-MOF (see Fig. 1d) and **kgd** network (with Schläfli symbol of $(4^3)_2(4^6.6^6.8^3))$[12] for 471-MOF (see Fig. 1i). The adjacent bilayers are parallel and isolated along *c*-axis in both isomers but with different arrangements, namely, $-(AB)_n-$ in 470-MOF (Fig. S8, ESI†) and $-(ABCDEF)_n-$ in 471-MOF (Fig. S9, ESI†). Although such stacking mode between the 2-D bilayers will significantly reduce the crossing window sizes in 470-MOF, 1-D channels are still observed along *c*-axis (Fig. 1e) with the effective sizes of 3.3 × 3.3 Å^2 (after considering the van der Waals radii). While the quadrangular meshes cannot be preserved along *c*-axis in 471-MOF for the stagger stacking mode for the 2-D bilayers. However, 1-D channels are formed along other two directions with the dimensions of 3.6 × 3.6 (see Fig. 1j) and 2.8 × 2.8 Å^2 (Fig. S10, ESI†) (after considering the van der Waals radii). The PLATON[13] analysis indicates that the effective free volumes are 42.4% (1566.4 Å^3) and 49.9% (6303.1 Å^3) per unit cell in 470-MOF and 471-MOF, respectively, after removing the lattice guest solvents. For such flexible coordination supramolecular systems, crystal transformations induced by solvent and temperature may occur.[14] In this work, both 470-MOF and 471-MOF are stable in hot dioxide, DMF, or their mixture, and will be unchanged at lower temperatures (Table S1, ESI†), revealing their thermodynamic stability in nature.

Gas sorption experiments were performed to further evaluate the difference of porosity for the two structures (Fig. S11, ESI†). Notably, both MOFs activated via heating or solvent-exchange will lose their crystallinity, which thus were treated by supercritical carbon dioxide drying (SCD) method (see Gas adsorption, ESI†) to properly remove the guest solvents before sorption measurements. Structural integrity of the activated samples can also be validated by the PXRD patterns (Fig. S12). The N_2 (77 K), Ar (87 K), and O_2 (87 K) uptakes for 470-MOF are quite low (Fig. 2a), while 471-MOF shows the type I isotherm with saturated uptakes of 122.0 cm^3 g^{-1} for N_2, 122.8 cm^3 g^{-1} for Ar, and 149.2 cm^3 g^{-1} for O_2 (Fig. 2e). As a result, the Brunauer–Emmett–Teller (BET) surface area is estimated to be 281.6 m^2 g^{-1} for 471-MOF while that for 470-MOF is only 7.0 m^2 g^{-1}. The adsorption isotherm for 470-MOF shows a 0.55 wt% (61.9 cm^3 g^{-1}) H_2 uptake at 77 K and 1 atm, while 471-MOF possesses a higher H_2 uptake of 0.73 wt% (81.8 cm^3 g^{-1}) under the same condition. The moderate H_2 uptakes for 470-MOF and 471-MOF are comparable to those (0.63–0.80 wt%) for the reported MOFs such as PCN-5,[15a] TUDMOF-2,[15b] SNU-15',[15c] and MOF-508.[15d] The sorption isotherms for both isomers at 195 K (Figs. 2b and 2f), 273 K (Figs. 2c and 2g), and 293 K (Figs. 2d and 2h) reveal that 470-MOF and 471-MOF have the maximum CO_2 uptakes over other gases (88.5 and 131.0 cm^3 g^{-1} at 195 K, 38.0 and 42.0 cm^3 g^{-1} at 273 K, and 27.4 and 25.6 cm^3 g^{-1} at 293 K). Notably, the CO_2 uptake of 471-MOF at 195 or 273 K is more than that of 470-MOF, while at 293 K, the maximum CO_2 uptake of 470-

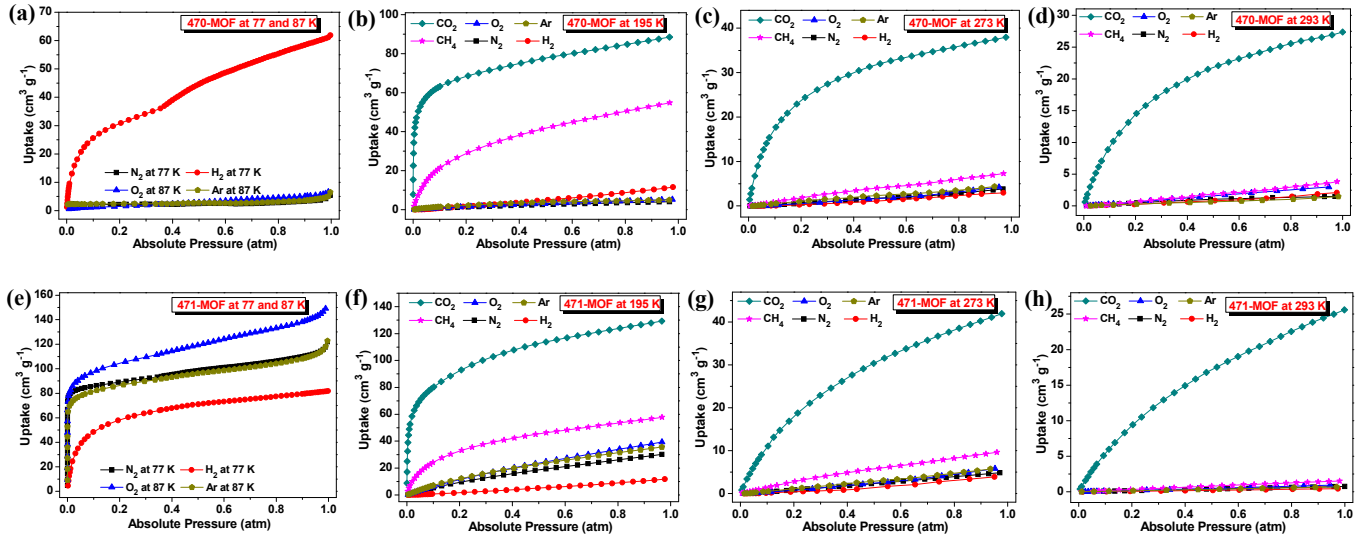

Fig. 2 Sorption isotherms of 470-MOF (a–d) and 471-MOF (e–h). N_2 and H_2 at 77 K; O_2 and Ar at 87 K (a, e). N_2, H_2, O_2, Ar, CH_4, and CO_2 at 195 K (b, f), 273 K (c, g), and 293 K (d, h).

Table 1 Calculated IAST selectivity (1 atm) for binary gas mixtures at 273 and 293 K.[a]

		CO_2/CH_4	CO_2/H_2	CO_2/O_2	CO_2/Ar	CO_2/N_2		CO_2/CH_4	CO_2/H_2	CO_2/O_2	CO_2/Ar	CO_2/N_2
273 K	470-MOF	2.7	6.2	4.6	4.4	5.3	471-MOF	1.4	3.3	2.3	2.6	2.7
293 K		3.2	6.0	3.9	8.9	7.6		4.5	15.7	7.0	10.0	9.3

[a] 15% for CO_2 and 85% for the other gas in each case.

MOF exceeds that of 471-MOF. The isosteric heats for CO_2 sorption calculated based on the adsorption data collected at 273 and 293 K,[16] indicate that the Q_{st} values for 470-MOF and 471-MOF are 35.4 and 20.8 kJ mol^{-1}, respectively. The high Q_{st} value for 470-MOF is comparable to those for known MOFs such as bio-MOF-1,[17a] TEA@bio-MOF-1 (TEA = tetraethylammonium),[17a] TMA@bio-MOF-1 (TMA = tetramethylammonium),[17a] PCN-6,[17b] MIL-53(Al),[17c] and HKUST-1.[17d] Meanwhile, 471-MOF shows a moderate Q_{st} value among those for MOFs, including CuBTTri,[18a] $Ni_2(BDC)_2(DABCO)$ (BDC = 1,4-benzenedicarboxylate; DABCO = triethylenediamine),[18b] $Zn_4(OH)_2$-(1,2,4-BTC)$_2$ (1,2,4-BTC = 1,2,4-benzenetricarboxylate),[18c] and Zn_2-(bpy)(TCM) (bpy = 4,4'-bipyridyl; TCM = tetrakis[4-(carboxyphenyl)-oxamethyl]methane).[18d] Further, we performed the IAST calculations and adsorption simulations for both isomers,[19] and the resulting IAST selectivity (Table 1) of CO_2 over other gases for 470-MOF and 471-MOF are in 2.7−6.2 and 1.4−3.3 at 273 K and 3.2−8.9 and 4.5−15.7 at 293 K, respectively. Interestingly, the adsorption selectivity at 293 K is higher than that at 273 K for all gases for 471-MOF, especially CO_2/H_2 and CO_2/Ar selectivity, while in the case of 470-MOF, only slight changes are observed for sorption selectivity at different temperatures. Moreover, at 273 K, the adsorption selectivity of 470-MOF is higher than that of 471-MOF for all gases, whereas at 293 K, the opposite results will be observed. Actually, the different sorption behaviors for 470-MOF and 471-MOF at lower temperatures (77 and 87 K) should be ascribed to the aperture size, where the smaller size for 470-MOF will allow fewer gas to be adsorbed, while those at 195 K can be attributed to both the aperture size and pore volume, that is, besides the above-mentioned point, the higher uptake of CO_2 for 470-MOF is caused by its larger pore volume. The sorption difference for CO_2 at 273 and 293 K may arise from the synergic influence of aperture size, pore volume, and host−guest interactions in both MOFs.[20] In fact, the smaller aperture size will usually lead to the higher sorption enthalpy, which indicates the stronger interactions between the coordination framework and CO_2. Therefore, the sorption amount of CO_2 decreases more slowly for 470-MOF against the temperature in comparison with that for 471-MOF.

In conclusion, we have synthesized two bilayer porous materials based on Co(II) and a flexible tricarboxylate ligand, which represent a pair of unique supramolecular isomers induced by the solvent templates. It should be noted that both structures have the similar Co(II) coordination geometry and ligand binding, and their subtle structural difference only originates from the arrangement and conformation of BTTB ligands and Co_3 SBUs. Further, their different porous features in crystallography can also be confirmed by their gas sorption behaviors at different temperatures. These results will offer more insights into the intricate structure-functionality relationship of porous MOFs and the rational design of new crystalline materials.

This work was supported by the National Natural Science Foundation of China (Nos. 21031002, 21171151, and 21201154), Plan for Scientific Innovation Talent of Henan Province, and the Program for Science & Technology Innovative Research Team in University of Henan Province (15IRTSTHN002).

Notes and references

[a] *Henan Provincial Key Laboratory of Surface & Interface Science, Zhengzhou University of Light Industry, Zhengzhou 450002, P. R. China*
[b] *College of Chemistry, Tianjin Key Laboratory of Structure and Performance for Functional Molecules, MOE Key Laboratory of Inorganic-Organic Hybrid Functional Material Chemistry, Tianjin Normal University, Tianjin 300387, China*
E-mail: shihz@zzuli.edu.cn, dumiao@public.tpt.tj.cn

† Electronic supplementary information (ESI) available: experimental details, TGA and PXRD plots, crystal structures (figures and tables), and gas adsorption. CCDC 1031076−1031081. For ESI and crystallographic data in CIF or other electronic format see DOI: 10.1039/c000000x/

1 (*a*) M. Du, C.-P. Li, M. Chen, Z.-W. Ge, X. Wang, L. Wang and C.-S. Liu, *J. Am. Chem. Soc.*, 2014, **136**, 10906–10909; (*b*) R. Grünker, V. Bon, P. Müller, U. Stoeck, S. Krause, U. Mueller, I. Senkovska and S. Kaskel, *Chem. Commun.*, 2014, **50**, 3450–3452; (*c*) M. Wriedt, J. P. Sculley, W. M. Verdegaal, A. A. Yakovenko and H.-C. Zhou, *Chem. Commun.*, 2013, **49**, 9612–9614.

2 (*a*) K. R. Meihaus, S. G. Minasian, W. W. Lukens Jr., S. A. Kozimor, D. K. Shuh, T. Tyliszczak and J. R. Long, *J. Am. Chem. Soc.*, 2014, **136**, 6056–6068; (*b*) K. S. Pedersen, J. Bendix and R. Clérac, *Chem. Commun.*, 2014, **50**, 4396–4415; (*c*) X. Feng, J. Liu, T. D. Harris, S. Hill and J. R. Long, *J. Am. Chem. Soc.*, 2012, **134**, 7521–7529.

3 (*a*) W. Zhang, G. Lu, C. Cui, Y. Liu, S. Li, W. Yan, C. Xing, Y. R. Chi, Y. Yang and F. Huo, *Adv. Mater.*, 2014, **26**, 4056–4060; (*b*) B. Gole, A. K. Bar, A. Mallick, R. Banerjee and P. S. Mukherjee, *Chem. Commun.*, 2013, **49**, 7439–7441; (c) A. Dhakshinamoorthy, A. M. Asiri and H. Garcia, *Chem. Commun.*, 2014, **50**, 12800–12814.

4 (*a*) X. Zhu, J. Gu, Y. Wang, B. Li, Y. Li, W. Zhao and J. Shi, *Chem. Commun.*, 2014, **50**, 8779–8782; (*b*) T. Kundu, S. Mitra, P. Patra, A. Goswami, D. D.#Díaz and R. Banerjee, *Chem.–Eur. J.*, 2014, **20**, 10514–10518; (*c*) Y. Wu, M. Zhou, S. Li, Z. Li, J. Li, B. Wu, G. Li, F. Li and X. Guan, *Small*, 2014, **10**, 2927–2936.

5 (*a*) R. Haldar, S. K. Reddy, V. M. Suresh, S. Mohapatra, S. Balasubramanian and T. K. Maji, *Chem.–Eur. J.*, 2014, **20**, 4347–4356; (*b*) L. Feng, Z. Chen, T. Liao, P. Li, Y. Jia, X. Liu, Y. Yang and Y. Zhou, *Cryst. Growth Des.*, 2009, **9**, 1505–1510; (*c*) F. Carson, J. Su, A. E. Platero-Prats, W. Wan, Y. Yun, L. Samain and X. Zou, *Cryst. Growth Des.*, 2013, **13**, 5036−5044; (*d*) D. Chen, Y.-J. Liu, Y.-Y. Lin, J.-P. Zhang and X.-M. Chen, *CrystEngComm*, 2011, **13**, 3827–3831.

6 B. Chen, N. W. Ockwig, F. R. Fronczek, D. S. Contreras and O. M. Yaghi, *Inorg. Chem.*, 2005, **44**, 181–183.

7 (*a*) S. Ghosh, S. Mukherjee, P. Seth, P. S. Mukherjee and A. Ghosh, *Dalton Trans.*, 2013, **42**, 13554–13564; (*b*) J.-M. Gu, S.-J. Kim, Y. Kim and S. Huh, *CrystEngComm*, 2012, **14**, 1819–1824; (*c*) J.-P. Zhang and S. Kitagawa, *J. Am. Chem. Soc.*, 2008, **130**, 907–917; (*d*) J.-P. Zhang, X.-L. Qi, C.-T. He, Y. Wang and X.-M. Chen, *Chem. Commun.*, 2011, **47**, 4156–4158; (*e*) C.-T. He, P.-Q. Liao, D.-D. Zhou, B.-Y. Wang, W.-X. Zhang, J.-P. Zhang and X.-M. Chen, *Chem. Sci.*, 2014, **5**, 4755–4762.

8 (*a*) T. Panda, P. Pachfule and R. Banerjee, *Chem. Commun.*, 2011, **47**, 7674–7676; (*b*) M. Chen, Y. Lu, J. Fan, G.-C. Lv, Y. Zhao, Y. Zhang and W.-Y. Sun, *CrystEngComm*, 2012, **14**, 2015–2023; (*c*) Y.-X. Hu, H.-B. Ma, B. Zheng, W.-W. Zhang, S. Xiang, L. Zhai, L.-F. Wang, B. Chen, X.-M. Ren and J. Bai, *Inorg. Chem.*, 2012, **51**, 7066−7074.

9 (*a*) X.-D. Chen, H.-F. Wu, X.-H. Zhao, X.-J. Zhao and M. Du, *Cryst. Growth Des.*, 2007, **7**, 124–131; (*b*) S. Ma, D. Sun, M. Ambrogio, J. A. Fillinger, S. Parkin and H.-C. Zhou, *J. Am. Chem. Soc.*, 2007, **129**, 1858–1859.

10 (*a*) B. Moulton and M. J. Zaworotko, *Chem. Rev.*, 2001, **101**, 1629–1658; (*b*) J. L. Atwood and J. W. Steed, *Encyclopedia of Supramolecular Chemistry*, CRC Press, London, 2004; (*c*) J.-P. Zhang, X.-C. Huang and X.-M. Chen, *Chem. Soc. Rev.*, 2009, **38**, 2385–2396.

11 (*a*) X.-M. Lin, T.-T. Li, Y.-W. Wang, L. Zhang and C.-Y. Su, *Chem. Asian J.*, 2012, **7**, 2796–2804; (*b*) X.-W. Wang, J.-Z. Chen and J.-H. Liu, *Cryst. Growth Des.*, 2007, **7**, 1227–1229; (*c*) Y. Hu, W. Zhang, X. Zhang, Z. Wang, Y. Li and J. Bai, *Inorg. Chem. Commun.*, 2009, **12**, 166–168.

12 M. O'Keeffe, see website: http://rcsr.net.

13 A. L. Spek, *J. Appl. Crystallogr.*, 2003, **36**, 7–13.

14 J.-P. Zhang, P.-Q. Liao, H.-L. Zhou, R.-B. Lin and X.-M. Chen, *Chem. Soc. Rev.*, 2014, **43**, 5789–5814.

15 (*a*) S. Ma, X.-S. Wang, E. S. Manis, C. D. Collier and H.-C. Zhou, *Inorg. Chem.*, 2007, **46**, 3432–3434; (*b*) I. Senkovska and S. Kaskel, *Eur. J. Inorg. Chem.*, 2006, 4564–4569; (*c*) Y. E. Cheon and M. P. Suh, *Chem. Commun.*, 2009, **45**, 2296–2298; (*d*) B. Chen, C. Liang, J. Yang, D. S. Contreras, Y. L. Clancy, E. B. Lobkovsky, O. M. Yaghi and S. Dai, *Angew. Chem., Int. Ed.*, 2006, **45**, 1390–1393.

16 (*a*) M. Dincă and J. R. Long, *J. Am. Chem. Soc*., 2005, **127**, 9376–9377; (*b*) S. Yang, X. Lin, A. J. Blake, G. S. Walker, P. Hubberstey, N. R. Champness and M. Schröder, *Nature Chem.*, 2009, **1**, 487–493; (*c*) J. I. Feldblyum, A. G. Wong-Foy and A. J. Matzger, *Chem. Commun.*, 2012, **48**, 9828–9830.

17 (*a*) J. An and N. L. Rosi, *J. Am. Chem. Soc.*, 2010, **132**, 5578–5579; (*b*) J. Kim, S.-T. Yang, S. B. Choi, J. Sim, J. Kim and W.-S. Ahn, *J. Mater. Chem.*, 2011, **21**, 3070–3076; (*c*) S. Bourrelly, P. L. Llewellyn, C. Serre, F. Millange, T. Loiseau and G. Férey, *J. Am. Chem. Soc.*, 2005, **127**, 13519–13521; (*d*) Q. M. Wang, D. Shen, M. Bülow, M. L. Lau, S. Deng, F. R. Fitch, N. O. Lemcoff and J. Semanscin, *Micropor. Mesopor. Mat.*, 2002, **55**, 217–230.

18 (*a*) A. Demessence, D. M. D'Alessandro, M. L. Foo and J. R. Long, *J. Am. Chem. Soc.*, 2009, **131**, 8784–8786; (*b*) Z. Liang, M. Marshall, A. L. Chaffee, *Micropor. Mesopor. Mat.*, 2010, **132**, 305–310; (*c*) Z. Zhang, S. Xiang, X. Rao, Q. Zheng, F. R. Fronczek, G. Qian and B. Chen, *Chem. Commun.*, 2010, **46**, 7205–7207; (*d*) P. K. Thallapally, J. Tian, M. R. Kishan, C. A. Fernandez, S. J. Dalgarno, P. B. McGrail, J. E. Warren and J. L. Atwood, *J. Am. Chem. Soc.*, 2008, **130**, 16842–16843.

19 (*a*) A. L. Myers and J. M. Prausnitz, *AIChE J.*, 1965, **11**, 121–127; (*b*) J. Duan, M. Higuchi, R. Krishna, T. Kiyonaga, Y. Tsutsumi, Y. Sato, Y. Kubota, M. Takata and S. Kitagawa, *Chem. Sci.*, 2014, **5**, 660–666; (*c*) M. H. Mohamed, S. K. Elsaidi, T. Pham, K. A. Forrest, B. Tudor, L. Wojtas, B. Space and M. J. Zaworotko, *Chem. Commun.*, 2013, **49**, 9809–9811.

20 Z. Zhang and M. J. Zaworotko, *Chem. Soc. Rev.*, 2014, **43**, 5444–5455.

